Sancho-Tello, M.; Forriol, F.; Martín De Llano, JJ.; Antolinos Turpín, CM.; Gómez-Tejedor, J.; Gómez Ribelles, JL.; Carda, C. (2017). Biostable scaffolds of polyacrylate polymers implanted in the articular cartilage induce hyaline-like cartilage regeneration in rabbits. The International Journal of Artificial Organs. 40(7):350-357. doi:10.5301/ijao.5000598

Biostable scaffolds of polyacrylate polymers implanted in the articular cartilage induce hyaline-like cartilage regeneration in rabbits

The International Journal of Artificial Organs 2017; 40(7): 350 - 357

DOI:10.5301/ijao.5000598

AUTHORS

María Sancho-Tello[1,2]*, Francisco Forriol[2,3], José J. Martín de Llano[1,2], Carmen Antolinos-Turpin[2,4], José A. Gómez-Tejedor[4,5], José L. Gómez Ribelles[4,5] , Carmen Carda[1,2,5]

[1]Departamento de Patología, Facultad de Medicina y Odontología, Universitat de València, Valencia, Spain.

[2]INCLIVA Biomedical Research Institute, Valencia, Spain.

[3]Hospital de la Malvarrosa, Valencia, Spain.

[4]Centre for Biomaterials and Tissue Engineering, Universitat Politècnica de València, Spain.

[5]Biomedical Research Networking Center on Bioengineering, Biomaterials and Nanomedicine (CIBER-BBN), Valencia, Spain.

***Corresponding author:**

María Sancho-Tello, MD, PhD

Departamento de Patología, Facultad de Medicina y Odontología, Universitat de València

Av. Blasco Ibáñez 15

E-46010 Valencia (Spain)

Telephone: (34)963952465

Fax Number: (34)963983226

E-mail: stello@uv.es

ABSTRACT

Purpose: To study the influence of scaffold properties on the organization of “in vivo” cartilage regeneration. Our hypothesis is that stress transmission to the cells seeded inside the scaffold pores or surrounding it, which is highly dependent on the scaffold properties, determine differentiation of both mesenchymal cells and dedifferentiated autologous chondrocytes.

Methods: Four series of porous scaffolds made of different polyacrylate polymers, previously seeded with cultured rabbit chondrocytes or without cells preseeded, were implanted in cartilage defects in rabbits. Subchondral bone was always injured during the surgery in order to allow blood to reach the implantation site and fill scaffold pores.

Results: Three months after implant, excellent tissue regeneration was obtained, with a well-organized layer of hyaline cartilage at the condylar surface in most cases of the hydrophobic or slightly hydrophilic series. The most hydrophilic material induced the poorest regeneration. However, few variations were observed between the preseeded and non-preseeded scaffolds. All the materials employed were biocompatible, biostable polymers, therefore, in contrast to other studies, our results are not perturbed by possible effects attributable to material degradation products, or to the loss of scaffold mechanical properties over time due to degradation.

Conclusions: Cartilage regeneration mainly depends on the properties of the scaffold, such as stiffness and hydrophility, whereas little differences were observed between preseeded and non-preseeded scaffolds.

KEYWORDS

Animal models; Biopolymers; Cartilage; Scaffolds; Tissue engineering.

INTRODUCTION

Articular cartilage has very limited ability to repair[1], therefore traumatic injuries, osteochondritis dissecans and degenerative processes lead to severe cartilage lesions eventually accompanied by pain, immobility, stiffness and progressive joint destruction. Different therapeutic strategies have been developed to prevent their progression, including tissue-response techniques like drilling[2], microfracture[3], osteochondral transplantation[4], and transplantation of periosteum or perichondrium to resurface damaged cartilage[1,5]. The results of these techniques are not always satisfactory, and thus microfracture-treated superficial defects remain unhealed[6], while full depth defects may heal with fibrocartilaginous tissue by recruiting mesenchymal stem cells from subchondral bone marrow[6,7]. Human autologous chondrocyte transplantation[8] has been successfully applied and is considered the gold standard in reparation of osteochondral injuries; however, its major disadvantages are a wide arthrotomy incision, the need to obtain enough cell number for large defects, and the fact that patients undergo two surgeries[7].

Tissue engineering techniques are leading to promising results in articular cartilage regeneration[9] by using empty scaffolds or seeded with autologous chondrocytes[10,11]. Scaffolds play important roles since they rapidly fill cartilage defects, provide a substrate where cells can adhere, and maintain mechanical integrity withstanding mechanical stresses. Therefore, they should be designed to match mechanical properties of native cartilage and support joint loading conditions[9,12,13].

Our aim was to compare “in vivo” cartilage regeneration by implanting scaffolds made of biostable materials with varying compliance, either preseeded with chondrocytes or non-preseeded, using series of polyacrylate polymer or copolymer networks, previously used in “in vitro” studies on cell adhesion and viability[14-18]. In

contrast to other studies[11,19,20], the materials we employed are biocompatible biostable polymers, thus our results are not perturbed by any effect attributable to material degradation products or to loss of mechanical properties over time due to scaffold degradation.

METHODS

Polymeric scaffolds

TABLE 1: Number of animals used per treatment group and compressive strength measurement of the scaffolds of the different series. Values are mean ± standard deviation of the Young's modulus (MPa).

Series	Composition	Number of animals		*E* (MPa)
		Non-preseeded	Preseeded	
I	P(EA-co-MAAc) 90/10	2	2	1.48±0.64
II	P(EA-co-HEA) 90/10	8	5	0.57±0.10
III	P(EA-co-HEA) 50/50	2	2	0.20±0.03
IV	PEA 100	8	5	2.24±0.73
Control		4		

Macroporous scaffolds were made of polymer or copolymer networks (Table 1): copolymers of ethyl acrylate, EA, and 10% methacrylic acid, MAAc [P(EA-co-MAAc)] (series-I); copolymers of EA and hydroxyethyl acrylate, HEA [P(EA-co-HEA)], containing 10% (series-II) or 50% (series-III) HEA; and poly(ethyl acrylate), PEA (series-IV). Triethyleneglycol dimethacrylate 5% (Aldrich, 98%) was used as cross-linking agent and 1% benzoin (Scharlau) as ultraviolet photosensitive initiator. Poly(methyl methacrylate; PMMA) microspheres (90μm average diameter) (Colacryl DP300, Lucite International) were used as scaffold templates, sintered under pressure above its glass transition temperature[15]. After polymerization, templates were dissolved with acetone for ~48h in a Soxhlet extractor, and immersed in large

excess of acetone, slowly changed to water in order to avoid scaffolds collapse. Scaffolds replicas were cut (~3mm diameter, 1mm thick), dried in vacuo for 24h at RT followed by 24h at 50ºC, and sterilized with gamma-radiation (25kGy) before used.

Series-I and II scaffolds are slightly hydrophilic (bulk polymers can absorb 2.3 and 3.3% of water, measured on dry basis when immersed in liquid water until equilibrium); series-III is a hydrogel whose equilibrium water content is 18.1% weight[16]; finally, series-IV is hydrophobic. Volume fraction of scaffold pores was 0.75±0.03 in all samples.

Scaffold morphology was examined by scanning electron microscope, SEM (JEOL-JSM6300)[10].

Scaffolds mechanical properties

Scaffold compressive strength was measured in a Thermo-Mechanical Analyzer (TMA-EXSTAR6000; Seiko Instruments) in control position mode with a 0.5-mm diameter stainless steel probe[10]. Cylindrical shape samples with 3.5mm diameter and 0.7mm thick were used for testing mechanical properties. Briefly, an initial 2% strain was applied for 15min; subsequently, 4 programs of compression loading up to 15% strain and unloading were performed at RT, both with a 20μm/min rate. Young's modulus was calculated from the slope of stress-strain curves in the linear region of the compression curve. Results are expressed as average value±standard deviation of a minimum of 5 measurements. Statistic has been analyzed using R software version 3.3.2.

Animals

Thirty-eight adult male New-Zealand rabbits, weighing ~1.5kg were obtained from Granjas San Bernardo (Tulebra). Quarantine lasted 7 days. Animals were housed in standard single cages under conventional conditions with appropriate bedding, controlled temperature and light, and provided free access to drinking water and food. The study protocol was approved by the Ethics Committee of the Universitat de València.

Rabbit chondrocyte harvesting and culture

In order to isolate chondrocyte, articular cartilage was obtained from knee joints of donor rabbits after their sacrifice with a lethal intravenous injection of 500mg Thiopental (Tiobarbital®, Braun)[10,14]. Briefly, cartilage was diced and successively incubated with enzymatic solutions. Isolated cells were diluted with Dulbecco's modified Eagle's medium (DMEM) supplemented with 10% fetal bovine serum (Invitrogen) and 50µg/ml ascorbid acid (Sigma-Aldrich), plated at high density, and cultured at 37ºC in a 5% CO_2 humidified atmosphere[14].

Scaffold were placed on a 24-well polystyrene culture plate, moistened with Hanks' Balanced Salt Solution (Sigma-Aldrich), and cell suspension (10^6 viable cells/20µl medium) was injected in the center of the scaffolds to allow cells to infiltrate the porous structure. After 1h incubation, scaffolds were changed to a new well and culture medium was gently added. After 3 days in culture, medium was replaced by DMEM containing 1% Insulin-transferrin-sodium-selenite media supplement (BD Biosciences) and 50µg/ml ascorbic acid, and scaffolds were cultured during 3 more days before implantation[10].

Scaffold implant

Scaffolds were implanted as previously published[10]. Briefly, rabbits were pre-anaesthetized by subcutaneous injection of 15mg/kg Ketamine (Ketolar®, Pfizer) and intramuscular injection of 0.1mg/kg Medetomina (Domtor®, Pfizer). General anesthesia was induced by 4% isofluorane and maintained with 1.5% isofluorane with O_2 (2l/min). Non-preseeded scaffolds were moistened with phosphate buffered saline (PBS), and vacuum was applied to assure liquid penetration into the pores. Knee joint arthrotomy was performed through a parapatellar incision and the patella laterally dislocated. A 3mm-trephine was used to create a chondral defect (3mm diameter, 1mm depth) in the central articulating surface of the femoral trochlear groove, injuring subchondral bone, thus allowing blood to flow towards the injury site. After rinsing with sterile saline, a scaffold was laid into the defect and held in place by repositioning the patella. Arthrotomy and skin were sutured. After surgery, analgesia and antibiotic prophylaxis was administered and rabbits were returned to their cages and allowed free cage activity.

Control animals received the same surgical procedure, including the 3mm-defect in the trochlea, but no scaffold was implanted.

The results observed after a first batch of animals (n=2 animals/group) were not satisfactory in series-I and III, therefore no additional animals were employed for these series, and only the number of animals of series-II, IV and controls were increased. Total number of animals/group is detailed in Table 1.

Animal sacrifice and tissue retrieval

After surgery, rabbits showed good general state, with no osteoarticular complication or infection, and normal activity. Three months after surgery, rabbits were sacrificed

as described above. Knee articular surface was observed and macroscopic pictures were taken.

Histological studies

Morphology was studied following standard histological procedures[10,11]. Briefly, articular specimens were fixed (4% formaldehyde, 5 days), and immersed in Osteosoft decalcifier solution (Merck) during 5-8 weeks. Then, samples were embedded in paraffin, 5µm-thick serial sections were obtained in the middle part of the scaffolds (~3mm diameter), and stained with hematoxylin-eosin and Masson's trichrome. Moreover, chondral glycosaminoglycan presence was monitored by alcian blue staining (pH 2.5), counterstained with Harris hematoxylin. Sections were analyzed under Leica-DM4000B optical microscope, and pictures were taken using a camera Leica-DFC420.

RESULTS

Figure 1a shows a representative scaffold observed with SEM, with a highly porous structure. Framework was studied in all series with higher magnification (Fig.1b-e), showing spherical interconnected pores with an average diameter around 60 µm without significant differences between samples, slightly smaller than the PMMA microspheres used as template (90µm). Pores presented an elliptical shape in P(EA-co-HEA) copolymers (Fig.1c,d) due to a certain scaffold collapse during solvent exchange from acetone to water during template extraction. Although pores were well interconnected in all series, throat size between pores was slightly smaller in series-I (Fig.1b).

Fig. 1: Scanning electron microscopy (SEM) of the scaffolds. (A) SEM cross-sectional image of P(EA-co-HEA) 50/50 (series III) scaffold. SEM pore structure images for all series: (B) series I, P(EA-co-MAAc) 90/10; (C) series II, P(EA-co-HEA) 90/10; (D) series III, P(EA-co-HEA) 50/50; and (E) series IV, PEA 100. Scale bars represent 500 µm (A) or 200 µm (b-e).

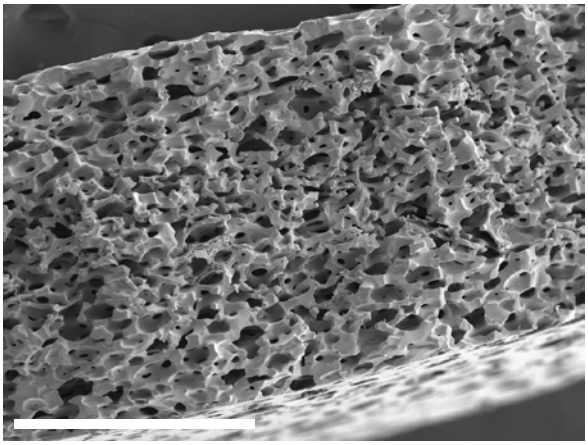

A

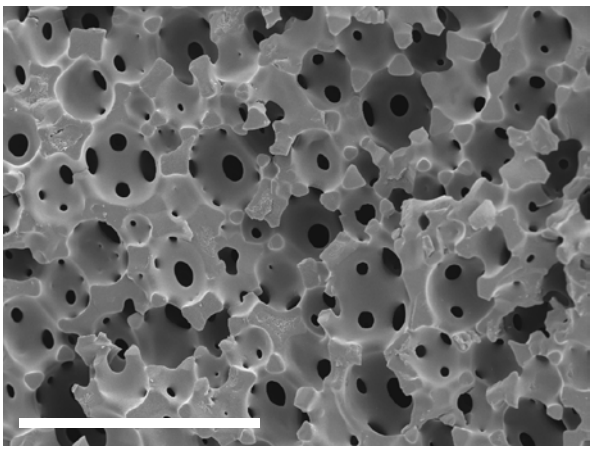

B

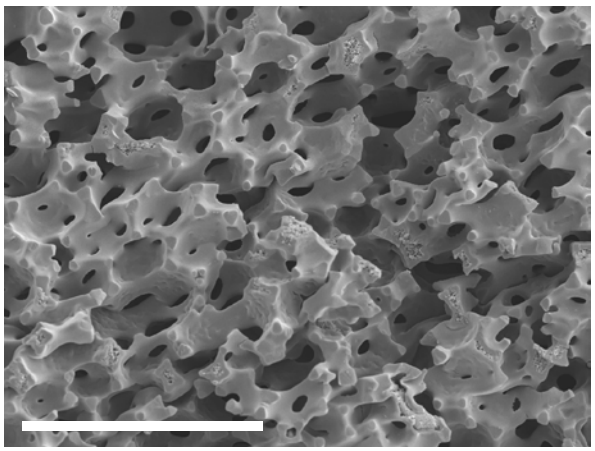

C

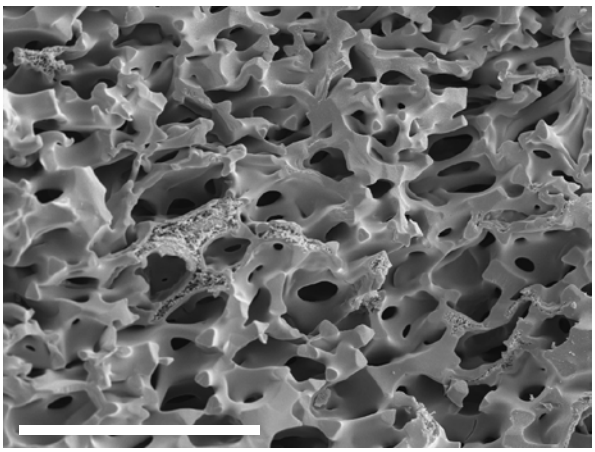

D

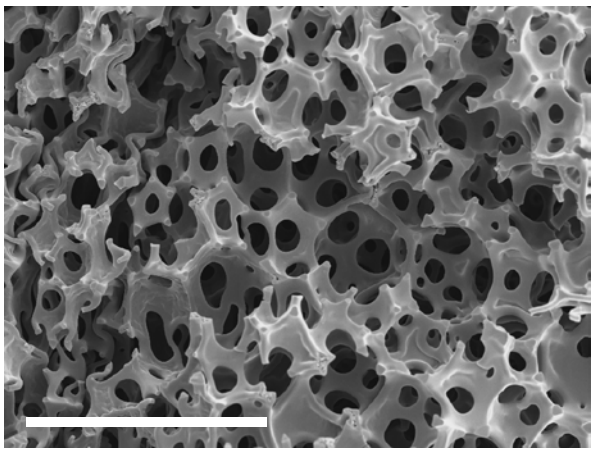

E

Scaffold Young's modulus showed the highest stiffness corresponding to pure PEA scaffold (Table 1). Copolymers containing HEA hydrophilic monomeric units presented a decreasing elastic modulus with increasing HEA content (series-II and III), as expected. These values were similar to those reported for cartilage in rabbits[20] (0.41±0.12 MPa), and humans[21] (0.58±0.17 MPa). On the contrary, scaffolds made of copolymers containing MMAc, that also provided certain hydrophilicity, had a stiffness close to pure PEA, which is ascribed to methyl group attached to MMAc, that imposes high energy barrier to the rotation of the main copolymer chain in P(EA-co-MMAc), thus tending to increase stiffness and balancing the effect of water sorption. The differences between Young moduli are statistically significant among them (p-value <0.05), except among sample I and IV.

Macroscopic observation at the implant zone after sacrifice revealed scaffolds smoothly covered by a thin translucent tissue with an apparent good integration into the osteoarticular complex, although a different aspect than the adjacent native cartilage was observed in all series, with a whiter color and a well-defined border (Fig.2).

Fig. 2: Representative macroscopic views of the articular surface of the different series, 3 months after scaffold implantation. Arrows show the injury zone of non-preseeded (A-D) or preseeded (E-H) series I to IV, respectively.

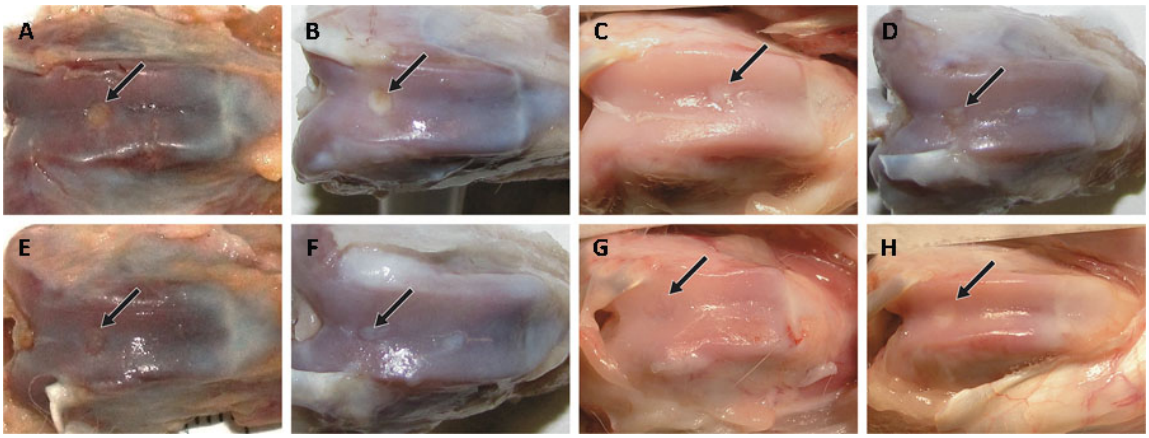

Fig. 3: Representative microscopic panoramic views of implanted scaffolds of non-preseeded (A-D) or preseeded (E-H) series I to IV, respectively, 3 months after implantation. Series I, II, and IV biomaterials were not stained and thus appeared as white spaces, while series III material appeared slightly stained gray (C, G). Sections were stained with Masson's trichrome (A, F, H), Alcian blue (B), or hematoxylin-eosin (C, D, E, G). Arrowheads show fibrous tissue. AC = articular cartilage; B = subchondral bone; S = scaffold. Scale bars represent 500 µm.

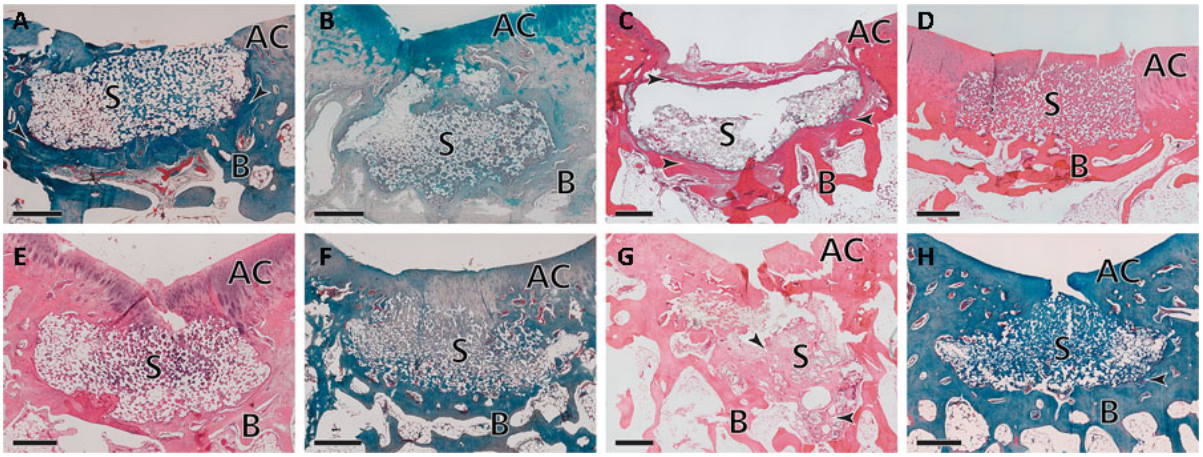

Microscopic analysis showed scaffolds preservation 3 months after implant (Fig.3), observed as white spaces in series-I, II and IV, or slightly stained in series-III, probably due to their hydrophilic properties.

Fig. 4: Different tissue responses to the implanted scaffolds, 3 months after implantation. (A) Non-preseeded scaffold series I contacts with the articular cavity. (B) Hyaline-like neocartilage grown on the surface of non-preseeded scaffold series II in continuity with native cartilage. (C) Good continuity between neocartilage grown within scaffold pores and surrounding superficial cartilage in preseeded series II. (D) Blood vessels (arrows) emerging from spongy bone tissue as well as good continuity between neotissue and subchondral bone in preseeded scaffold series II. (E) Abundant fibrous tissue (arrowheads) with numerous giant multinuclear phagocytic cells (star) inside and around the implanted preseeded scaffold series III, where the biomaterial is stained gray (S). (F) Synovial-like tissue (asterisk) over the implanted scaffold in non-preseeded series IV. Sections were stained with Masson's trichrome (A, D, E), Alcian blue (B), or hematoxylin-eosin (C, F). AC = articular cartilage; B = subchondral bone; S = scaffold. Scale bars represent 100 µm.

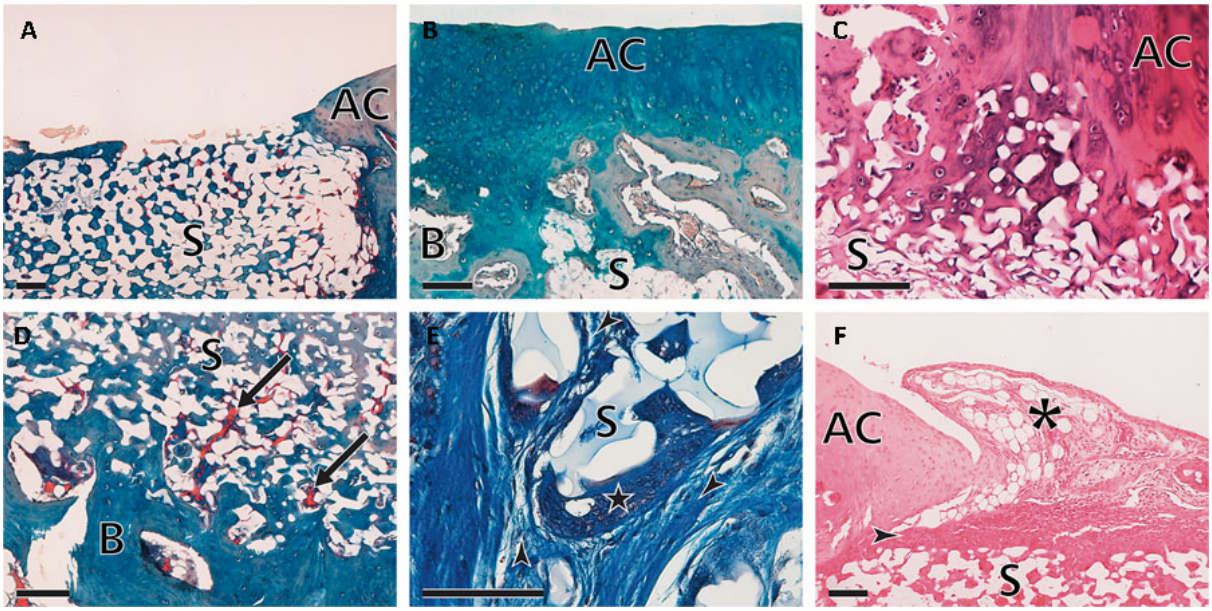

Series-I had a mild, irregular response (Figs.3a,3e), with a neosynthesized superficial cartilage covering most of scaffold surface; some samples were located away from the surface, whereas others were near it and presented areas in direct contact with the articular cavity (Fig.4a). This material induced irregular scaffold integration within the osteoarticular complex, with well-integrated zones while other areas were surrounded by fibrous tissue. Colonization by neotissue was mild in preseeded samples and poorer in non-preseeded ones.

Series-II induced the best response (Figs.3b,3f), with a regenerated articular surface resembling hyaline cartilage in all samples (Fig.4b). They presented a good integration in the osteoarticular complex (Figs.4c,4d), although small areas surrounded by connective tissue were eventually observed. Scaffold pores were densely populated by neotissue in non-preseeded samples and even more abundant in preseeded ones, that was avascular hyaline cartilage occupying the upper and middle parts of the scaffolds (Fig.4c), whereas in the lower part it resembled bone tissue, containing mesenchymal and osteoblast-like cells along with blood vessels (Fig.4d).

Series-III presented the worst response (Figs.3c,3g). Superficial cartilage neoformation was mild in some samples but presented areas of fibrosis. Abundant dense fibrous tissue surrounded and frequently invaded all scaffolds, containing numerous giant multinucleated phagocytic cells (Fig.4e). Moreover, neotissue formation inside the scaffolds was almost absent in both preseeded and non-preseeded samples.

Series-IV had also a good response (Figs.3d,3h), although the reparative response seemed slower than in series-II. Scaffolds were often close to the articular surface (in 8 out of 13 samples), and some presented areas in direct contact with this cavity and

eventually synovial-like tissue (Fig.4f), as it was also observed in some series-I and III samples. Although a tendency of a closer location of the scaffold to the articular surface was observed in series IV (247 ± 190 μm) with respect to other series, no statistically significant difference was found ($p>0.05$). However, a high coefficient for a negative correlation was observed ($R^2 = 0.982$) when Young's modulus was plotted against the scaffold distance to the articular surface (Fig. 5).

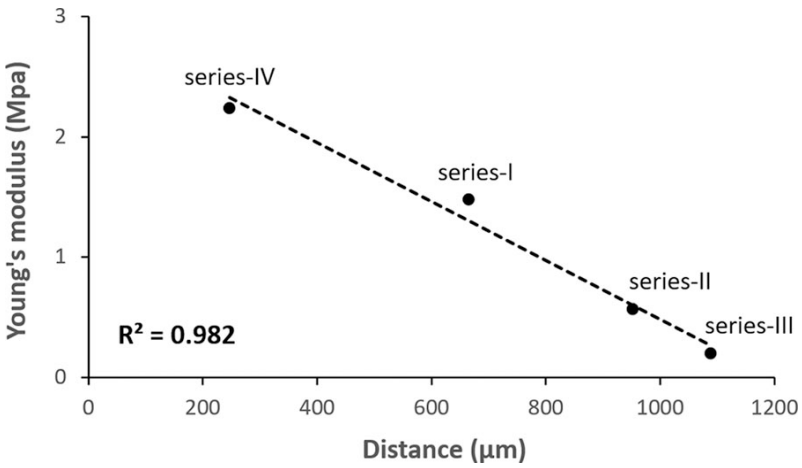

Fig. 5: Linear regression between Young's modulus and scaffold distance from articular surface in the series studied. A high negative correlation coefficient

Series IV showed good integration with the osteoarticular complex although small areas of fibrosis surrounding scaffolds were also present. Neotissue grown inside scaffold pores was abundant in both non-preseeded and preseeded samples (445 ± 160 cells/mm2 vs. 330 ± 234 cells/mm2, respectively, with no statistically significant difference), with a similar morphological pattern to series II (cartilage in the top, bone tissue in the bottom).

Finally, control animals (Fig. 6), which underwent the same surgical procedure but where no scaffold was implanted, showed neotissue filling the chondral defect with macroscopic characteristics similar to those with scaffolds. However, microscopic analysis revealed the presence of fibrous tissue covering the whole defect.

Fig. 6: Control samples. Representative macroscopic view of the articular surfaces (A) and microscopic views (B, inset C), 3 months after surgery. Sections were stained with Masson's trichrome (B, C). Arrow shows the injury zone and arrowhead fibrous tissue. AC = articular cartilage; B = subchondral bone. Scale bars represent 500 µm (b) or 100 µm (c).

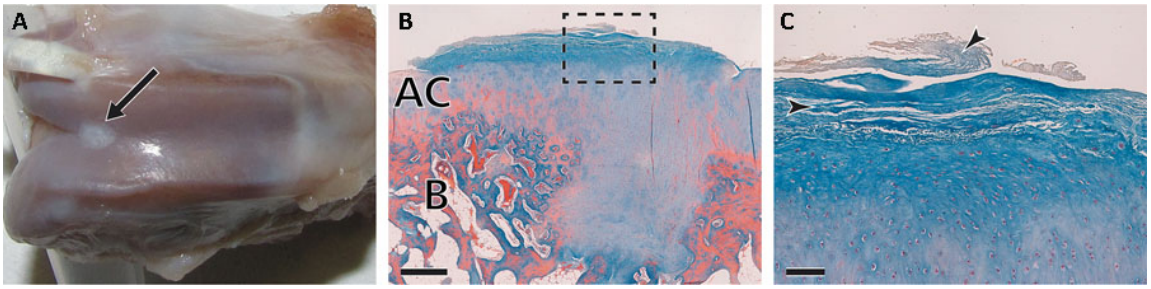

DISCUSSION

We showed in a previous study[10] that implanting a scaffold made of P(EA-co-HEA), series II, in a rabbit knee model, yielded the formation of hyaline cartilage, and thus the aim in this work was to determine the effect of scaffold compliance on tissue regeneration by increasing stiffness by substituting the hydrophilic component, HEA, by MAAc (series I) or by PEA (series IV), or on the contrary increasing compliance by increasing the HEA content (series III). We observed that cartilage-like neotissue covered scaffolds 3 months after implantation, and also that neotissue occupied scaffold pores in both preseeded and non-preseeded samples, but the quality of the neotissue depended on the nature of the material implanted. Implantation was accompanied by blood flow at the injury zone because we wounded the subchondral bone. Because no statistically significant difference was found between neotissue growth inside scaffolds in preseeded and non-preseeded scaffolds, our results suggest that neotissue originated primarily from the differentiation of mesenchymal cells that invaded the scaffold, whereas native cartilage around the lesion also

participated in the neoformation of articular cartilage, that actively proliferated, as reported in a 1-year evolution study using series II scaffolds[10]. When non-preseeded scaffolds were implanted, they immediately absorbed blood, even the most hydrophobic material (PEA), because their pores were filled with PBS before implantation. It is worth remarking that the scaffolds occupied the defect tightly and they were level with the surrounding condylar surface.

The behavior of invading cells and the tissue characteristics they generated clearly depended on the scaffold properties. It is well known that mesenchymal cells, recruited from subchondral bone marrow in microfracture-treated cartilage full defects, acquire chondrogenic phenotype and produce cartilaginous extracellular matrix (ECM), which frequently degenerates into fibrocartilage[3]. Our innovation is that we filled the defect with a polymeric scaffold, modifying mechanical loading state to which cells were subjected, showing the important effect of the biomechanics at the defect site during regeneration on the neotissue quality. If subchondral bone is microfractured but the defect site is kept empty, a layer of cartilage is formed 3 months after implant, but regenerated tissue did not fully occupy the defect site[20]. Those cells located at the defect site are not subjected to compression loading, which is totally withstood by the non-injured surrounding cartilage.

However, when scaffolds filled the defect site, cells located at the condylar surface over the scaffold are subjected to compressive stresses and react by producing cartilaginous ECM. The neotissue generated had hyaline cartilage characteristics: isolated cells in lacunae forming perpendicular columns to the surface, and a cartilaginous ECM (Figs.3b,3f,4b). Obviously, the biomechanics at the surface is highly dependent on the material elastic modulus, whereas the ability to grow in depth of the regenerated superficial cartilage depends on the scaffold deformability.

Besides, mesenchymal cells that invaded the scaffold porous structure and produced ECM, continuously increased the elastic modulus of the scaffold-cell construct. In fact, in control samples, where no scaffold was implanted and therefore no compressive stresses were transmitted to surrounding tissue, a highly fibrous neotissue was observed filling and covering the excavated lesion (Figs.5b,5c), as previously observed[10].

Implant location 3 months after surgery seemed the result of a competition between two forces: on the one hand, the growth in depth of regenerated cartilage on top of the material, which deformed the scaffold and pushed it downward, and on the other hand, the increased resistance of the scaffold bulk itself due to the regenerated tissue in its pores[10]. This fact can explain the different scaffold locations observed as a function of the material elasticity. Thus, PEA, the stiffest material, seemed unaltered in its primitive location and showed the thinnest layer of hyaline cartilage on top (Fig.3d), while the hydrogel P(EA-co-HEA)50/50, much softer due to its hydrophilicity, was often deformed and compressed in subchondral bone (Fig.3g). This latter material not only lacked regenerated tissue within its pores, but also induced a highly reactive fibrosis around it (Fig.4e). The behavior of series-I and II, of average stiffness, were intermediate, with a thick layer of hyaline cartilage covering the scaffold (Figs.3b,3e,3f).

The biological response also depended on the scaffold chemical composition. P(EA-co-MAAc) copolymer contains acid groups in the MAAc unit, that dissociates in aqueous medium leaving negative electrical charges attached to the polymer chain, which was favorable for several cell types “in vitro”[16-18], but “in vivo” response was poor, since only a mild colonization was observed along with fibrotic areas partly surrounding both preseeded and non-preseeded scaffolds (Figs.3a,3e).

On the other hand, P(EA-co-HEA) copolymers contains hydroxyl groups in the side chains of the polymer backbone, that increases water absorption capacity and diminishes “in vitro” cell attachment[14,16,17], which did not correlate with “in vivo” response. Thus, series-II and IV, which showed the best performance, had scaffold pores filled with abundant cells isolated in lacunae (Fig.4c). We want to remark that we previously showed the presence of proliferative cells in series-II scaffolds[10]. Given the poor proliferating nature of “in vivo” adult chondrocytes, these results suggest that cells colonizing scaffold came from the proliferation of both mesenchymal cells and preseeded chondrocytes. The scarce number of cells inside P(EA-co-HEA)50/50 scaffold (Figs.3c,3g), could be due to the lack of cell attachment mentioned above, and/or to the collapse of these soft scaffolds due to compressive forces exerted by the tissue growing on top of the surface, that pushed the scaffold towards subchondral bone.

Morphological comparison of the regenerated tissue between non-preseeded and preseeded scaffolds shows similar general characteristics. The main difference is a higher number of cells within preseeded scaffolds, as expected. The tissue that occupies scaffold pores resembles hyaline cartilage, with cells isolated in lacunae and an ECM containing specific cartilage components[10]. At least part of these cells are probably originated by mesenchymal cells invading the scaffold, as in non-preseeded scaffolds discussed above, but the increased colonization observed within them strongly suggests that seeded dedifferentiated chondrocytes were also able to originate “in vivo” hyaline-like tissue.

No significant differences were observed in the regenerated tissue over scaffold surface between preseeded or non-preseeded ones, suggesting that the regeneration mechanism is the same, and it essentially depends on the mechanical

characteristics of the material rather than on the presence or absence of preseeded cells. In fact, when polycaprolactone scaffolds were used in a protocol similar to ours but avoiding any injure of subchondral bone (thus preventing blood flow at the implantation site), no top layer of hyaline cartilage was observed 3 months after implantation, although scaffold pores showed cartilaginous tissue[20].

In conclusion, hyaline-like cartilage was regenerated in rabbit articular defects 3 months after implanting porous scaffolds, and morphological differences were observed between the diverse series as a function of their stiffness and hydrophilicity. Good scaffold integration was observed in the host tissue, although scaffolds with lower stiffness appeared protruded towards subchondral bone and covered by an upper layer of hyaline-like tissue, whereas stiffer scaffolds were mainly located closer to the articular surface and the neotissue invading its pores, was hyaline-like cartilage in the scaffold middle and upper parts, while bone-like tissue and ingrowth of vessels were observed in the lower part. These findings were similar in non-preseeded scaffolds and in those preseeded with “in vitro” expanded chondrocytes, but with a denser cellularity in the preseeded ones. It suggests that the regenerated tissue is mainly originated by the differentiation of mesenchymal cells that arrived from subchondral bone as a consequence of the surgical procedure, and differentiate towards hyaline chondrocytic phenotype in a process strongly dependent on the transmission of mechanical stresses to the cells. Thus, the critical role of the scaffold is to guarantee cell exposure to a mechanical environment capable to withstand immediate compression forces and to transmit them to the cells from the very first moment after surgery, triggering their differentiation towards the chondrocytic lineage, which is important in the design of scaffolds for cartilage regeneration.

ACKNOWLEDGEMENTS

The authors gratefully acknowledge the financial support from the Ministry of Economy and Competitiveness through project No. MAT2013-46467-C4-R, including the FEDER financial support, with complementary funding of Generalitat Valenciana with projects ACOMP/2009/112 and ACO, and Universitat Politècnica de València with 2911-2008 projects. CIBER-BBN is an initiative funded by the VI National R&D&I Plan 2008-2011, Iniciativa Ingenio 2010, Consolider Program. CIBER Actions are financed by the Instituto de Salud Carlos III with assistance from the European Regional Development Fund.

The authors are grateful to “Servicio de Microscopía Electrónica” of Universitat Politècnica de València for their valuable help, to R. García Gómez for technical assistance in the scaffolds preparation and to J. Benavent in the histological techniques.

REFERENCES

1. Nelson L, Fairclough J, Archer CW. Use of stem cells in the biological repair of articular cartilage. Expert Opin Biol Ther. 2010;10(1):43-55.
2. Insall J. The Pridie debridement operation for osteoarthritis of the knee. Clin Orthop Relat Res. 1974;101:61-67.
3. Steadman JR, Rodkey WG, Briggs KK, Rodrigo JJ. The microfracture technic in the management of complete cartilage defects in the knee joint. Orthopade. 1999;28(1):26-32.
4. Hangody L, Kish G, Kárpáti Z, Udvarhelyi I, Szigeti I, Bély M. Mosaicplasty for the treatment of articular cartilage defects: application in clinical practice. Orthopedics. 1998;21(7):751-756.
5. Minas T, Nehrer S. Current concepts in the treatment of articular cartilage defects. Orthopedics. 1997;20(6):525-538.
6. Steinwachs MR, Guggi T, Kreuz PC. Marrow stimulation techniques. Injury. 2008;39(Suppl 1):S26-S31.
7. Richter W. Mesenchymal stem cells and cartilage in situ regeneration. J Intern Med. 2009;266(4):390-405.
8. Brittberg M, Lindahl A, Nilsson A, Ohlsson C, Isaksson O, Peterson L. Treatment of deep cartilage defects in the knee with autologous chondrocyte transplantation. N Engl J Med. 1994;331(14):889-895.
9. Ahmed TA, Hincke MT. Strategies for articular cartilage lesion repair and functional restoration. Tissue Eng Part B Rev. 2010;16(3):305-329.
10. Sancho-Tello M, Forriol F, Gastaldi P, et al. Time evolution of in vivo articular cartilage repair induced by bone marrow stimulation and scaffold implantation in rabbits. Int J Artif Organs. 2015;38(4):210-223.

11. Vikingsson L, Sancho-Tello M, Ruiz-Saurí A, et al. Implantation of a polycaprolactone scaffold with subchondral bone anchoring ameliorates nodules formation and other tissue alterations. Int J Artif Organs. 2015;38(12):659-666.
12. Little CJ, Bawolin NK, Chen X. Mechanical properties of natural cartilage and tissue-engineered constructs. Tissue Eng Part B Rev. 2011;17(4):213-227.
13. Vikingsson L, Gallego Ferrer G, Gómez-Tejedor JA, Gómez Ribelles JL. An “in vitro” experimental model to predict the mechanical behavior of macroporous scaffolds implanted in articular cartilage. J Mech Behav Biomed Mater. 2014;32:125-31.
14. Pérez Olmedilla M, Garcia-Giralt N, Pradas MM, et al. Response of human chondrocytes to a non-uniform distribution of hydrophilic domains on poly (ethyl acrylate-co-hydroxyethyl methacrylate) copolymers. Biomaterials. 2006;27(7):1003-1012.
15. Diego RB, Olmedilla MP, Aroca AS, et al. Acrylic scaffolds with interconnected spherical pores and controlled hydrophilicity for tissue engineering. J Mater Sci Mater Med. 2005;16(8):693-698.
16. Campillo-Fernandez AJ, Pastor S, Abad-Collado M, et al. Future design of a new keratoprosthesis. Physical and biological analysis of polymeric substrates for epithelial cell growth. Biomacromolecules. 2007;8(8):2429-2436.
17. Campillo-Fernández AJ, Unger RE, Peters K, et al. Analysis of the biological response of endothelial and fibroblast cells cultured on synthetic scaffolds with various hydrophilic/hydrophobic ratios: influence of fibronectin adsorption and conformation. Tissue Eng Part A. 2009;15(6):1331-1341.

18. Soria JM, Sancho-Tello M, Esparza MA, et al. Biomaterials coated by dental pulp cells as substrate for neural stem cell differentiation. J Biomed Mater Res A. 2011;97(1):85-92.

19. Izquierdo R, Garcia-Giralt N, Rodriguez MT, et al. Biodegradable PCL scaffolds with an interconnected spherical pore network for tissue engineering. J Biomed Mater Res Part A. 2008;85(1):25-35.

20. Martinez-Diaz S, Garcia-Giralt N, Lebourg M, et al. In vivo evaluation of 3-dimensional polycaprolactone scaffolds for cartilage repair in rabbits. Am J Sports Med. 2010;38(3):509-519.

21. Jurvelin JS, Buschmann MD, Hunziker EB. Mechanical anisotropy of the human knee articular cartilage in compression. Proc Inst Mech Eng H. 2003;217(3):215-219.

Table 1. Number of animals used per treatment group and compressive strength measurement of the different series. Values express the mean value ± standard deviation of the Young's modulus (Mpa).

Series	**Composition**	**Number of animals**		***E* (Mpa)**
		non-preseeded	preseeded	
I	P(EA-co-MAAc) 90/10	2	2	1.48 ± 0.64
II	P(EA-co-HEA) 90/10	8	5	0.57 ± 0.10
III	P(EA-co-HEA) 50/50	2	2	0.20 ± 0.03
IV	PEA 100	8	5	2.24 ± 0.73
control		4	-	

FIGURE LEGENDS

Figure 1. Scanning electron microscopy (SEM) of the scaffolds. (a) SEM cross-section image of P(EA-co-HEA) 50/50 (series-III) scaffold. SEM pore structure images for all series: (b) series-I, P(EA-co-MAAc) 90/10; (c) series-II, P(EA-co-HEA) 90/10; (d) series-III, P(EA-co-HEA) 50/50; and (e) series-IV, PEA 100. Scale bars represent 500 µm (a) or 200 µm (b-e).

Figure 2. Representative macroscopic views of the articular surfaces of the different series, 3 months after scaffold implant. Arrows shows the injury zone of non-preseeded (a-d), or preseeded (e-h) series-I to IV, respectively.

Figure 3. Representative microscopic panoramic views of implanted scaffolds of non-preseeded (a-d), or preseeded (e-h) series-I to IV, respectively, 3 months after implantation. Series-I, II and IV biomaterials were not stained and thus appeared as white spaces, while series-III material appeared slightly stained in gray (c,g). Sections were stained with Masson’s trichrome (a,f,h), alcian blue (b) or hematoxylin-eosin (c,d,e,g). Arrowheads show fibrous tissue; AC = articular cartilage; B = subchondral bone; S = scaffold. Scale bars represent 500 µm.

Figure 4. Different tissue response to the implanted scaffolds, 3 months after implantation. (a) Non-preseeded scaffold series-I contacts with the articular cavity. (b) Hyaline-like neocartilage grown on the surface of non-preseeded scaffold series-II. (c) Good continuity between neocartilage grown within scaffold pores and surrounding superficial cartilage in preseeded series-II. (d) Blood vessels (arrows)

emerging from spongy bone tissue as well as a good continuity between neotissue and subchondral bone in preseeded scaffold series-II. (e) Abundant fibrous tissue (arrowheads) with numerous giant multinuclear phagocytic cells (star) inside and around the implanted preseeded scaffold series-III, where biomaterial is stained in gray (S). (f) Synovial-like tissue (asterisk) over the implanted scaffold in non-preseeded series-IV. Sections were stained with alcian blue (b), Masson's trichrome (a, d, e), or hematoxylin-eosin (c, f). AC = articular cartilage; B = subchondral bone; S = scaffold. Scale bars represent 100 µm.

Figure 5. Control samples. Representative macroscopic view of the articular surfaces (a) and microscopic views (b, inset c), 3 months after surgery. Sections were stained with Masson's trichrome (b, c). Arrow shows the injury zone and arrowhead fibrous tissue. AC = articular cartilage; B = subchondral bone. Scale bars represent 500 µm (b) or 100 µm (c).